How do drops evaporate?

N. Murisic and L. Kondic

Department of Mathematical Sciences,

Center for Applied Mathematics and Statistics,

New Jersey Institute of Technology, Newark, NJ 07102

(Dated: February 21, 2008)

Abstract

We consider evaporation of pure liquid drops on a thermally conductive substrate. Two evaporative models are considered: one that concentrates on the liquid phase in determining evaporative flux, and the other one that centers on the gas/vapor phase. A single governing equation for the evolution of drop thickness, including both models, is developed. Experiments are used to estimate relevant parameters. We show how the derived governing equation can be used to predict which evaporation model is appropriate under considered experimental conditions.

PACS numbers: 68.03.Fg,68.15.+e,47.55.Ca,47.55.np

Evaporating thin films and drops are present in numerous natural situations and applications of technical importance. Coated liquid films, for example, are often left to dry by evaporation. The residual films, whose thickness may vary from millimetric in the case of paints to nanometric for photoresist films in semiconductor applications, are often desired in a uniform state. However, various kinds of instabilities, many of them driven by evaporation-related mechanisms, often occur. Evaporative sessile drops are perhaps even more interesting since nonuniform drop thickness and presence of contact lines (separating liquid, gas, and solid phase) lead to new effects. One of these is a possibility of nonuniform evaporation along the gas-liquid interface, leading to temperature gradients and related Marangoni effects. These effects are crucial in a number of problems, including the so-called coffee-stain phenomenon involving deposition of solid particles dissolved in the liquid close to a contact line [1], and its' numerous applications, such as analysis of DNA microarrays [2].

Despite its apparent simplicity, the problem of an evaporating drop on a thermally conducting solid substrate involves a number of physical processes, including mass and energy transfer between the three phases, diffusion and/or convection of vapor in the gas phase, coupled to the complex physics in the vicinity of a contact line. So-called '2-sided' models include the processes both in the liquid and in the gas phase, but lead to a mathematical formulation of significant complexity, even when the solid phase and contact line issues are not considered [3]. Therefore, most of the researchers in the field have chosen to use various simplifications, allowing them to reduce the complete problem to a tractable mathematical formulation. As we discuss below, these simplifications are based on estimating the importance of various physical processes, and lead eventually to models which concentrate on the processes in one of the phases (gas or liquid). The estimates, however, involve quantities which are either not known, or not known precisely enough. We will show that various assumptions may lead to models which can produce qualitatively different and contradictory results. The answer to the question 'How do drops evaporate?' is still not known.

The complete 2-sided model can be simplified by realizing that thermal conductivity and viscosity of vapor are small compared to the ones of the liquid. In addition, assuming that the gas phase is convection-free, one reduces the 2-sided model to the so-called '1.5-sided' model which includes the processes in the liquid, and the diffusion of vapor in the surrounding air [4]. An estimate of a typical diffusion time scale $t_d = l^2/D$, involves the relevant thickness of the gas phase, l, and the diffusion constant for e.g. water vapor $D \approx 10^{-5}\, m^2/s$. Assuming

for a moment that l is on millimeter scale (comparable to a typical thickness of a drop), leads to $t_d \approx 10^{-2}\ s$. The argument that t_d is much shorter than a typical time scale involved in drop evolution has been used to reduce the diffusion equation for vapor concentration, c, to a Laplace equation [5]. Furthermore, assuming that evaporation process itself is extremely fast [6] allows to completely ignore the processes in the liquid for the purpose of finding the mass flux. Therefore, the problem is simplified to $\nabla^2 c = 0$ in the gas/vapor domain. Concentrating now on the part of domain close to the contact line, one realizes electrostatic analogy of finding an electric field (mass flux, J) in the vicinity of a 'lens' shaped conductor (the drop), where c plays the role of electrostatic potential [1]. Typically this lens model assumes a pinned (stationary) contact line, although this assumption is not crucial since typically the contact line, even if mobile, evolves slowly [7]. One important outcome of the model is that, under some additional simplifications, $J \propto 1/h^{\lambda}$, where h is the drop thickness, and $\lambda = \lambda(\Theta)$, Θ being the contact angle [8]. Clearly, J diverges at the contact line, and various (often ad-hoc) procedures have been used to regularize the problem. An extensive modeling using lens-type model has been carried out, implementing both finite-element and lubrication- type approaches [5, 9]. Various versions of this model have been used to predict evaporative behavior of alcane [10] and colloidal drops [8, 11] and the temperature along liquid-gas interface [12], among others.

Turning now to the liquid phase, one realizes that the evaporation is limited by two physical processes: heat diffusion through the liquid supplying heat to the interface, and evaporation itself. In a simple model [3], these two processes can be related via Biot's number, $Bi = Kp_T L d_0/(\rho_v k)$, where $K = \alpha\rho_v(T_i)/\sqrt{2\pi R_g T_{sat}}$ and $p_T = Lp_{sat}/(R_g T_{sat}^2)$. Here, p_{sat} is the saturation pressure, R_g is the universal gas constant divided by the molar mass, L is the latent heat of vaporization, d_0 is drop thickness, ρ_v is vapor density, k is liquid heat conductivity, T_i and T_{sat} are the interface and saturation temperatures, and α is the accommodation coefficient, describing probability of phase change. The limit $Bi \to 0$ implies that the temperature of the liquid/gas interface tends to the temperature of the solid, evaporation itself proceeds in reaction-limited regime, and the interface is in a state of non-equilibrium [3]. $Bi \to \infty$, on the other hand, indicates that the evaporation is much faster than the heat diffusion through the liquid, and evaporation proceeds in liquid heat diffusion-limited regime, with the interface being in an equilibrium state.

While most of the quantities entering the definition of Bi are well known, the value of

α is questionable. A variety of α's in the range $O(1) - O(10^{-6})$ have been used in the literature, often without much justification. We note that the theoretical predictions that $\alpha \in [10^{-2}, 1]$ for water have been found to grossly overestimate the volatility, with values in the range $[10^{-6}, 10^{-4}]$ being more realistic [13]. In our experiments described below, we find $\alpha \approx 10^{-6}$, consistently with other experimental results involving drops exposed to open atmosphere [13]. This α gives $Bi \approx 10^{-2}$, suggesting that evaporation proceeds in the reaction-limited regime. Further insight can be reached by considering Bi as the ratio of the relevant time scales involved in heat diffusion in the liquid, t_l, and the one related to the evaporative process itself, t_e. Using $t_l = {d_0}^2/\kappa$, where κ is thermal diffusivity of liquid, and $d_0 = 0.5\ mm$, one finds $t_l \approx 1 sec$, giving $t_e \approx 10^2\ sec$. Similar value is obtained by using $t_e = (2\rho d_0 L)/(k\Delta T)$, where ΔT is the appropriate temperature scale [14]. Since $t_e \gg t_l \gg t_d$, one may consider a model where relevant limiting mechanism is the evaporative process itself, and not the diffusion of vapor in the gas. This 'non-equilibrium one sided' (NEOS) model has been extensively used for a variety of problems involving evaporative thin films [15], but only few works have applied it to evaporating drop problem [11, 14, 16]. We note that the argument outlined here for use of the NEOS model is based on the assumption of relatively small relevant thickness, l, governing diffusion in the gas phase. Larger l would lead to larger t_d, and thus it would be unclear which model is more appropriate. We note that, if t_d is large, the assumption of steady-state formulation for the gas concentration is questionable.

In this letter we show computationally that these two commonly used models for evaporation may lead to inconsistent results regarding volume loss, time evolution of the drop size, and in particular regarding the temperature gradient along the liquid-gas interface. We show that each model requires the use of unknown quantities, making it difficult to decide on which one is more appropriate. Therefore, we carry out experiments to estimate these quantities and compare the two models, with the goal of reaching a conclusion regarding an appropriate one, at least for the experiments considered. To our knowledge, this is the first time these two models have been compared directly against each other using data appropriate to a particular experiment.

The mathematical model consists essentially of Navier-Stokes equations for the liquid phase coupled with the energy equation for the solid, and appropriate expression for J, in the spirit of the models reviewed in [15]. We use lubrication approximation although for

some considered problems (such as a dionized water (DIW) drop on a silicon (Si) substrate) the contact angle is relatively large ($\Theta \approx 40^\circ$). This approach is supported by finite-element simulations that show that even for large contact angles considered here, lubrication approach leads to reliable results [5]. Solid-liquid interaction is included using disjoining pressure model with both attractive and repulsive van der Waals (vdW) terms, leading to a stable equilibrium thickness, which can be related to commonly used precursor film. In cylindrical coordinates and assuming azimuthal symmetry, we obtain the following 4th order PDE for the film thickness, $h(r,t)$

$$\begin{aligned}
&\frac{\partial h}{\partial t} + EJ + \frac{S}{r}\left[rh^3\left(h_{rrr} + \frac{1}{r}h_{rr} - \frac{1}{r^2}h_r\right)\right]_r - \\
&\frac{E^2}{rD}\left[rJh^3J_r\right]_r + \frac{M}{rP}\left[rh^2\left(h+\mathcal{W}\right)J_r\right]_r + \frac{M}{rP}\left[rJh^2h_r\right]_r \\
&+\frac{A}{r}\left[rh^3\left(\left(\frac{b}{h}\right)^3 - \left(\frac{b}{h}\right)^2\right)_r\right]_r + \frac{G}{r}\left[rh^3h_r\right]_r = 0\,,
\end{aligned} \tag{1}$$

which is put in nondimensional form by choosing d_0 and d_0^2/ν as the length and time scale, respectively (ν is the kinematic viscosity). We used a similar formulation to consider instabilities of evaporative isopropyl alcohol (IPA) drops [14]. The main difference of the present case (in addition to the geometry) is keeping the evaporative flux $J(h)$ explicitly in the formulation, so that Eq. (1) can be used for any evaporative model. Eq. (1) includes the effects due to viscosity, evaporation, capillarity, vapor recoil, Marangoni and vdW forces, and gravity. All nondimensional quantities are defined in [14], and here we just enumerate the most important ones: E, S, M, P, A, G correspond to evaporation number, nondimensional surface tension, Marangoni number, Prandtl number, nondimensional Hamaker constant, and gravity. The material parameters are listed in [14].

Next we concentrate on the key point, and that is the evaporative flux, J. For the lens model, we use $J(h) = \chi/h^\lambda$, where the exponent λ can be approximated by $\lambda = 0.5 - \Theta/\pi$ [5]. For the NEOS model, we use $J(h) = 1/(h + \mathcal{W} + \mathcal{K})$ [14], where $\mathcal{W}$ accounts for finite thermal conductivity of the solid substrate and $\mathcal{K} = Bi^{-1}$. For the case of DIW, $\mathcal{K}$ is typically large, as discussed before, and therefore $J(h)$ only weakly depends on h. The crucial parameters, volatility χ and α are obtained from the experiments described next.

The experiments are carried out at room temperature and in open atmosphere, using a goniometer (KSV CAM 200) which consists of a camera, light source, and static deposition

platform. Pure liquids and silicon wafers of semiconductor grade smoothness are used. Figure 1a) shows an example of an image of evaporating DIW drop. The build-in software analyzes the images and yields the height and the radius of a drop. Figure 1b) shows the resulting radius and volume of evaporating drop as a function of time. In agreement with other works, we find linear decrease of the volume for the considered time interval [5, 8, 18]. We note that we do not observe either significant stick-slip motion, nor contact line pinning that is often assumed to occur [5, 9]. Possibly, these effects are not seen due to small surface roughness of the Si wafers and due to purity of the liquids.

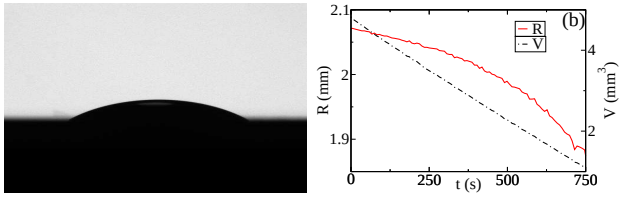

FIG. 1: (a) Snapshot of evaporating DIW drop on Si substrate; (b) Volume and radius of the drop as a function of time (experimental results).

In order to extract χ and α from the experimental data, we proceed as follows. The considered experimental time frame (typically the first 106 *sec*), is split into subintervals, and then the mass loss in each subinterval is used to obtain appropriate values of χ and α by integrating J over the drop surface (more details regarding this procedure will be given elsewhere [17]). We expect that this method is more accurate than simply using the dry out time to estimate the flux, since at late stages of evolution, the evaporation rate may be reduced [18]. Figure 2 shows the results. For the purpose of verification, we have applied the same approach to the already available experimental data [5] and obtained similar values for α and χ. With these values available, we are now almost ready to proceed with numerical simulations of the drop evolution governed by Eq. (1). The only missing ingredient is the precursor film thickness, b. Although it is typically sufficient to use $b \ll 1$, here we are more careful since quantitative agreement is desired. We are governed by the requirement that $r(t)$ and $V(t)$ should not depend on b in any significant manner, and have found that for $d_0 b \leq 0.625\ \mu m$ this requirement is satisfied. Coincidentally or not, this value is consistent with the equilibrium adsorbed film thickness $d_0 b_e$ for which evaporation stops due to attracting vdW forces [16]. For the appropriate parameters, we find $d_0 b_e \approx 0.5\ \mu m$. We note that consideration of vdW forces automatically regularizes otherwise singular expression

for J in the lens model [19]. Without inclusion of vdW effects, an additional externally added regularization of J has to be included in order to correctly compute the total mass flux.

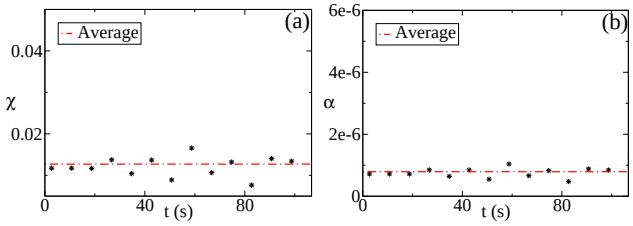

FIG. 2: Volatility for (a) lens and (b) NEOS models for DIW/Si, leading to $\alpha \approx 0.8 \cdot 10^{-6}$ and $\chi \approx 1.3 \cdot 10^{-2}$ (lines).

The numerical simulation of Eq. (1) is carried out using second order accurate implicit scheme which is an extension of the one used in [14] to cylindrical geometry. All simulations use as an initial condition the steady-state solution of Eq. (1) obtained by removing the evaporative terms; in experiments, this configuration is reached after a very short time. Figure 3a) shows the volume of the evaporating drop as a function of time. We find very good agreement between the experimental results and the NEOS model, while the lens model overestimates the volume loss due to evaporation. Therefore we conclude that, at least for the problem considered, the NEOS model predicts better the volume loss compared to the lens model. We discuss this difference, as well as additional experiments/simulations involving evaporation on different solid surfaces and under modified experimental conditions elsewhere [17].

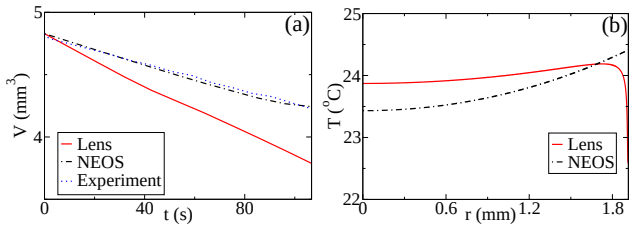

FIG. 3: (a) Volume of an evaporating DIW drop: comparison of the models with the experiment. (b) Temperature of the liquid-gas interface predicted by the two models at the final time shown in (a).

Figure 3b) shows that the two models predict qualitatively different temperature profiles along the liquid-gas interface. An increase of temperature as one moves from the center

in the NEOS model is the consequence of the fact that the heat supplied from the solid is larger than the heat loss due to evaporation. The lens model, on the other hand, predicts significantly larger evaporative flux in the contact line region, therefore leading to a sharp decrease of temperature. An increase of temperature as one moves away from the drop center is consistent with the results [12, 20] obtained using the lens model, and similar values of Θ and thermal conductivities of the liquid and solid, although under the assumption of a pinned contact line. However, the results presented here predict a 'stagnation point', where the temperature gradient changes sign. Presence of a stagnation point, although based on different physical grounds, was discussed earlier as one of the necessary ingredients required for formation of ring-like deposits occurring during evaporation of colloidal drops [8]. We note that simulations assuming the lens model for smaller values of Θ lead to monotonically decreasing temperatures along the liquid-gas interface as one moves away from the drop center, in full agreement with the earlier results [12, 20].

Next, we apply these two models to a more volatile IPA drop. This configuration is characterized by $\Theta \approx 6^\circ$ leading to very thin drops. Due to this fact, in our experiments we cannot follow accurately the evolution in the manner it was done for DIW drops. Therefore, we use the dryout time, which we can estimate with a reasonable accuracy, to obtain the required values of α and χ. For $V(0) \approx 3.2\ mm^3$, we find $t_{dry} \approx 135\ sec.$ Applying the two evaporative models leads to $\alpha = 2.5 \cdot 10^{-6}$ and $\chi = 4.6 \cdot 10^{-2}$. We note that similar values of χ were obtained in experiments with pure alcanes [10]. Implementing these values, we solve Eq. (1) using the parameters appropriate for IPA and Si [14].

Figure 4a) show the resulting evolution of the drop radius, $R(t)$, and the temperature along the liquid-gas interface (b). First, we notice dramatically different evolution of $R(t)$ for the two models. Considering the temperature profiles in 4b) provides immediate understanding of this difference. The Marangoni forces act in the opposing directions, leading to a very different evolution. For example, for the lens model, the Marangoni forces act outwards, leading to initial increase of the drop radius (shown in Fig. 4a) despite the loss of mass due to evaporation. The difference between the temperature profiles predicted by the two models is much more significant in the case of IPA compared to DIW due to its larger volatility. We discuss the details of model predictions regarding evolution of IPA drops in more details elsewhere [17].

We find it intriguing that the two commonly used models for evaporation produce results

that are qualitatively different, regarding the evolution of drops' volume, radius, and, in particular, the liquid-gas interfacial temperature. The resulting Marangoni forces may act in the opposing directions. Therefore, it appears that the arguments involving, e.g., the influence of Marangoni forces on formation of particle deposits next to the contact line have to be carefully reconsidered. We hope that the results presented here will encourage more elaborate experiments, possibly involving direct measurement of the interfacial liquid-gas temperature, an ultimate test for any evaporation model.

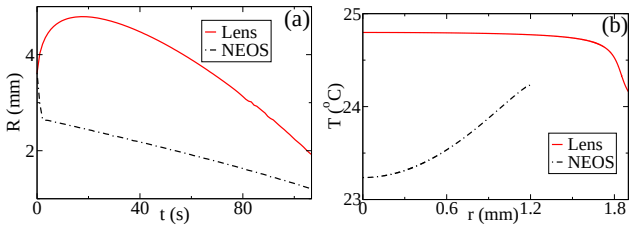

FIG. 4: IPA drop: (a) Radius $R(t)$ as a result of the two models; (b) Temperature profiles of the liquid-gas interface at the final time shown in (a).

Acknowledgments. We thank Pierre Colinet, Javier Diez, Yehiel Gotkis, Alex Oron, Bill Ristenpart, and Howard Stone for useful discussions.

[1] R. Deegan *et al.*, Nature **389**, 827 (1997).

[2] R. Blossey, Nature Materials **2**, 301 (2003).

[3] P. Colinet, J. Legros, and M. Velarde, *Nonlinear dynamics of surface-tension-driven instabilities* (Wiley-VCH, Berlin, 2001).

[4] J. Margerit, M. Dondlinger, and P. Dauby, J. Colloid Interface Sci. **290**, 220 (2005).

[5] H. Hu and R. Larson, J. Phys. Chem. B **106**, 1334 (2002).

[6] Y. O. Popov, Phys. Rev. E **71**, 036313 (2005).

[7] M. Cachile *et al.*, Langmuir **18**, 8070 (2002).

[8] R. Deegan *et al.*, Phys. Rev. E **62**, 756 (2000).

[9] H. Hu and R. Larson, Langmuir **21**, 3963 (2005).

[10] G. Guena, C. Poulard, and A. Cazabat, Colloids and Surfaces A **298**, 2 (2007).

[11] B. Fischer, Langmuir **18**, 60 (2002).

[12] W. Ristenpart *et al.*, Phys. Rev. Lett. **99**, 234502 (2007).

[13] R. Marek and J. Straub, Int. J. Heat Mass Transfer **44**, 39 (2001).

[14] Y. Gotkis *et al.*, Phys. Rev. Lett. **97**, 186101 (2006).

[15] A.Oron, S. H. Davis, and S. G. Bankoff, Rev. Mod. Phys. **69**, 931 (1997).

[16] V. Ajaev, J. Fluid Mech. **528**, 279 (2005).

[17] N. Murisic and L. Kondic (2007), in preparation.

[18] R. Deegan, Phys. Rev. E **61**, 475 (2000).

[19] S. Saritha and P. Neogi, Phys. Fluids **19**, 112104 (2007).

[20] H. Hu and R. Larson, Langmuir **21**, 3972 (2005).

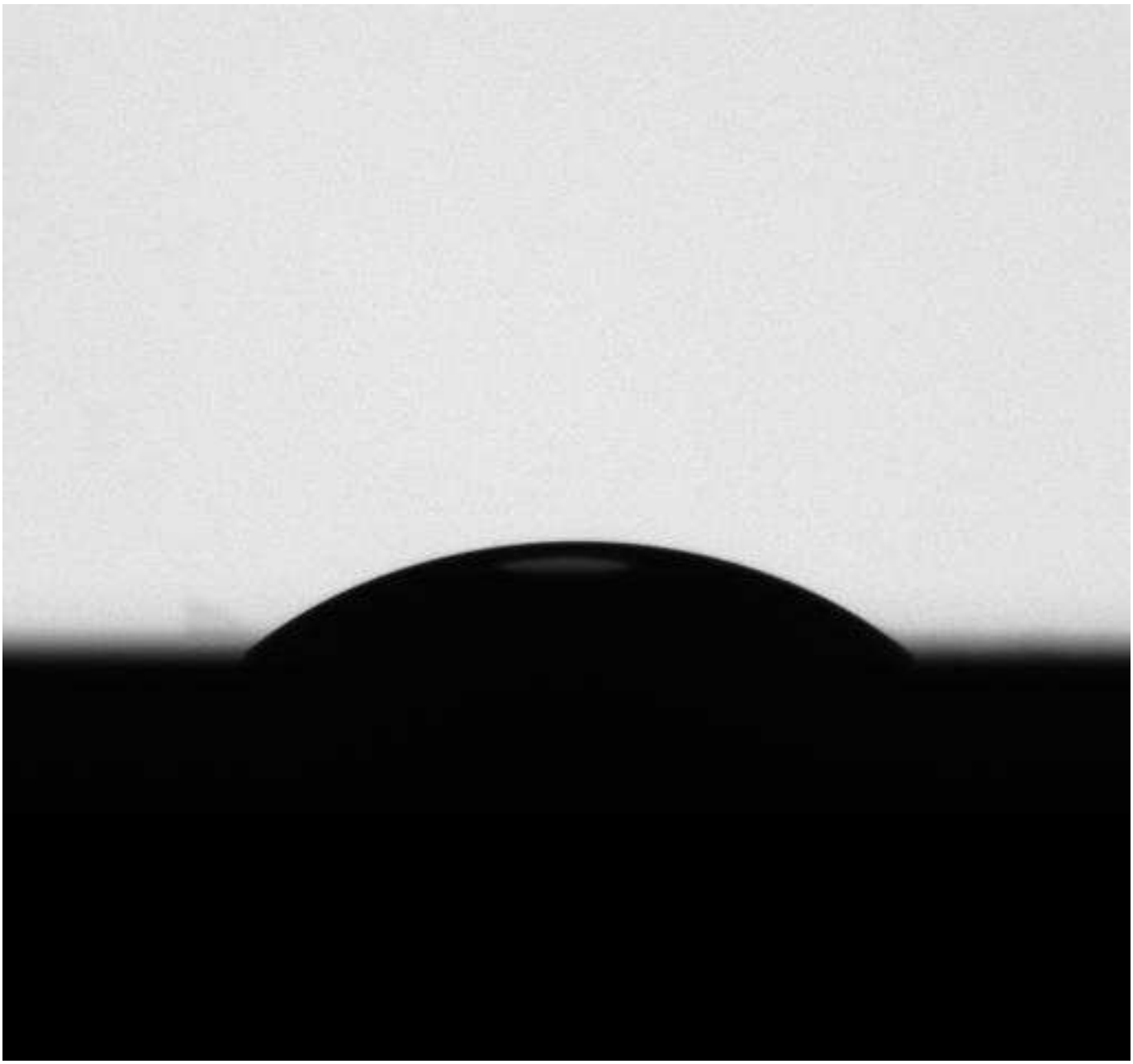

Figure 1a

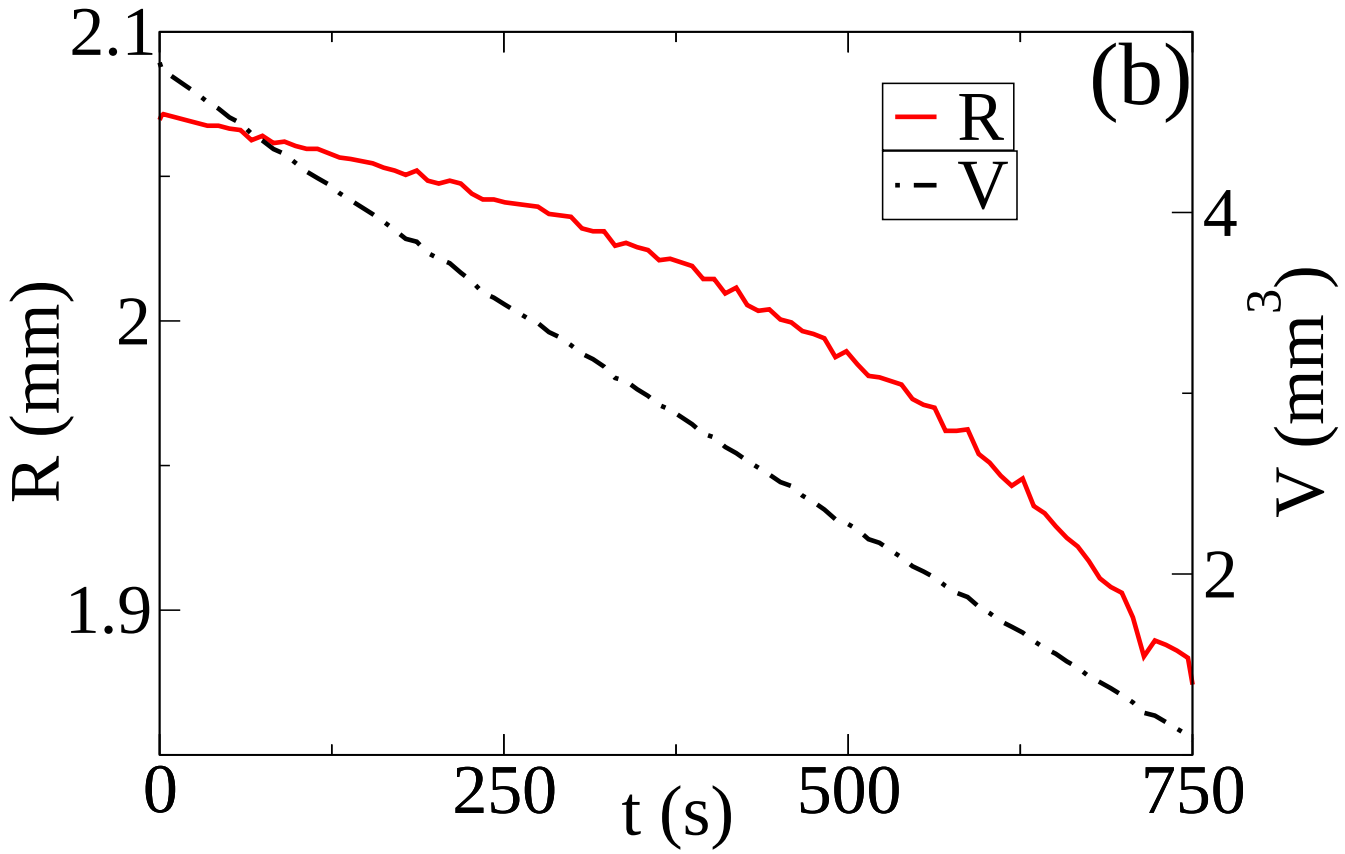

Figure 1b

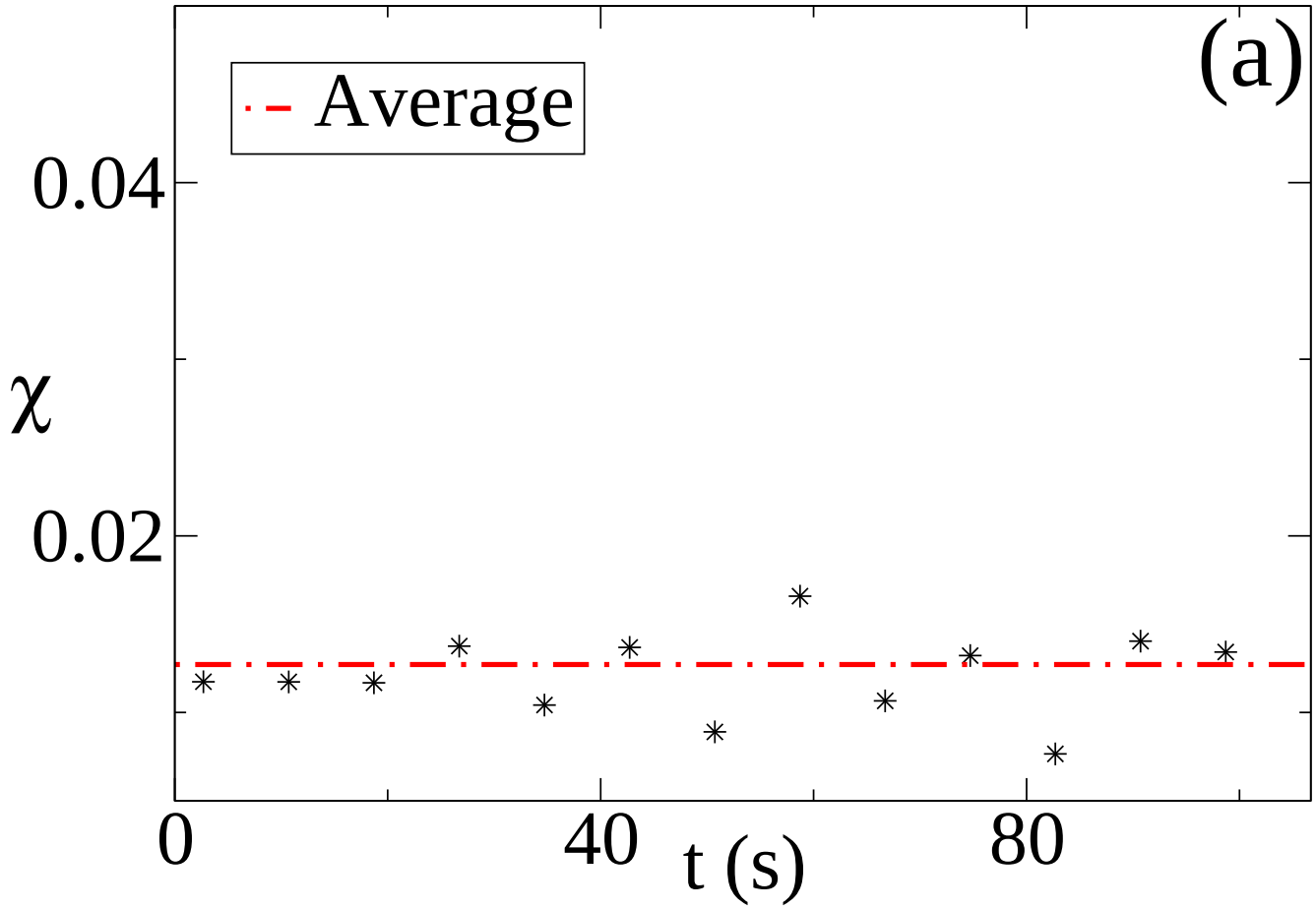

Figure 2a

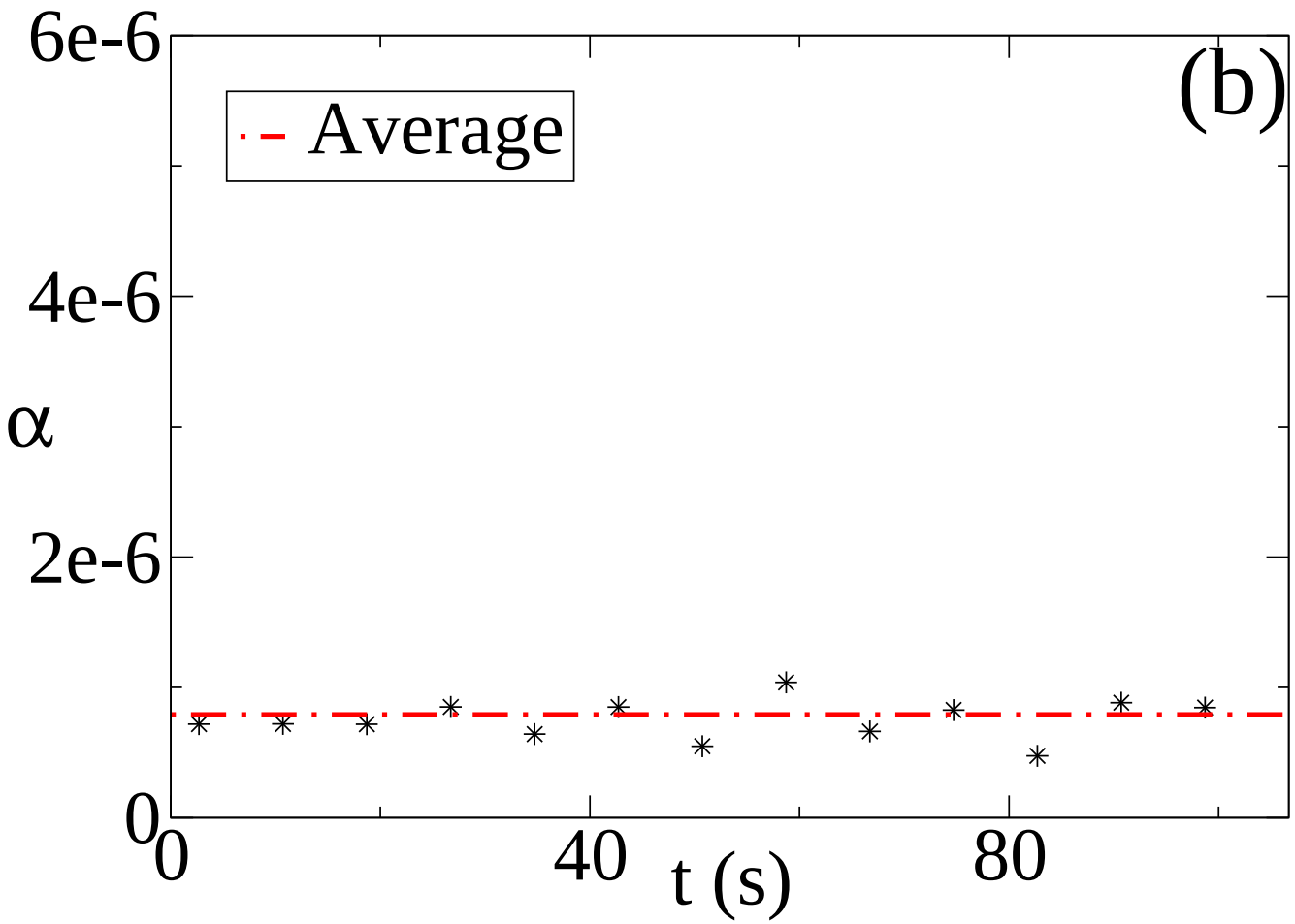

Figure 2b

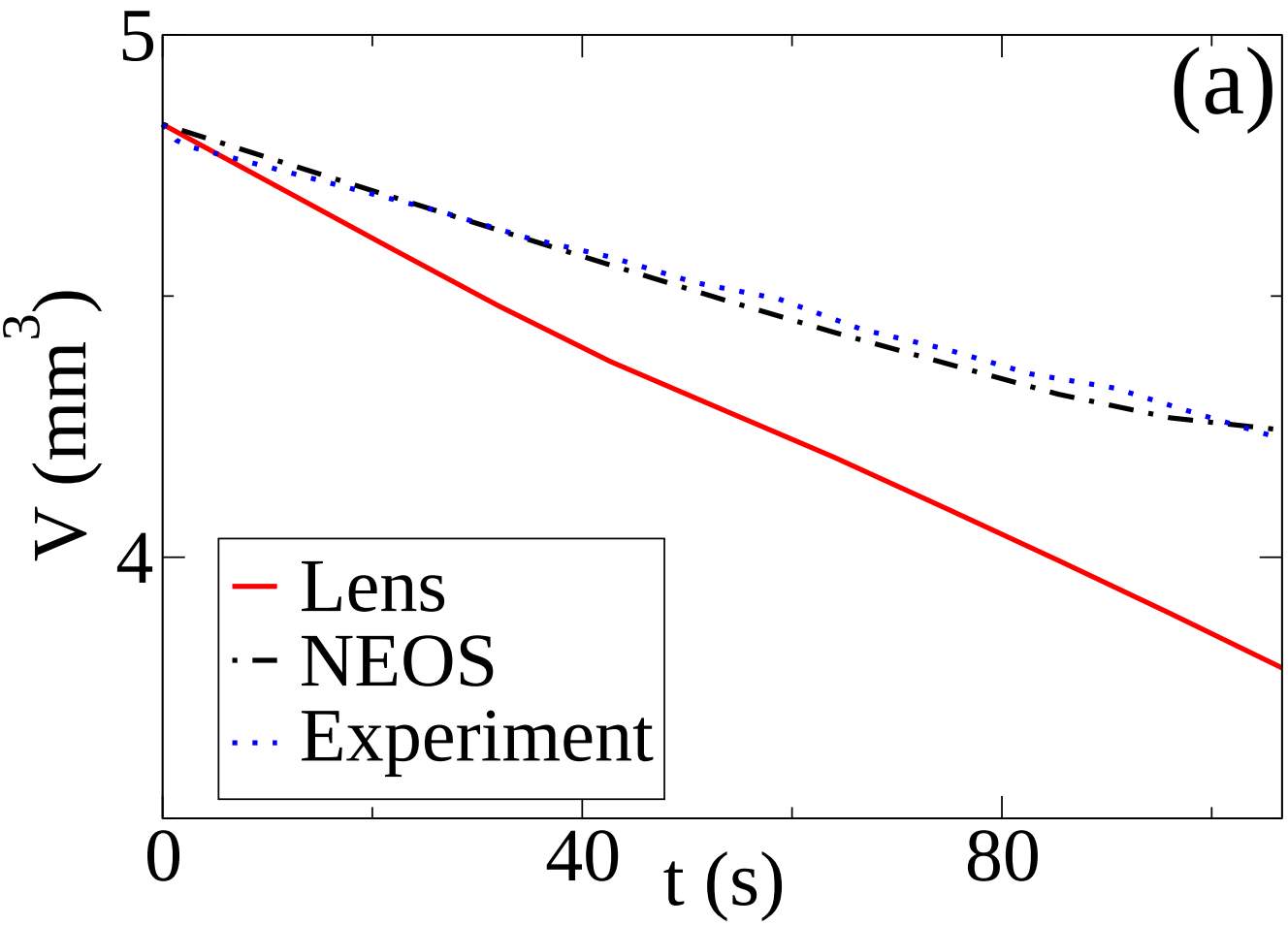

Figure 3a

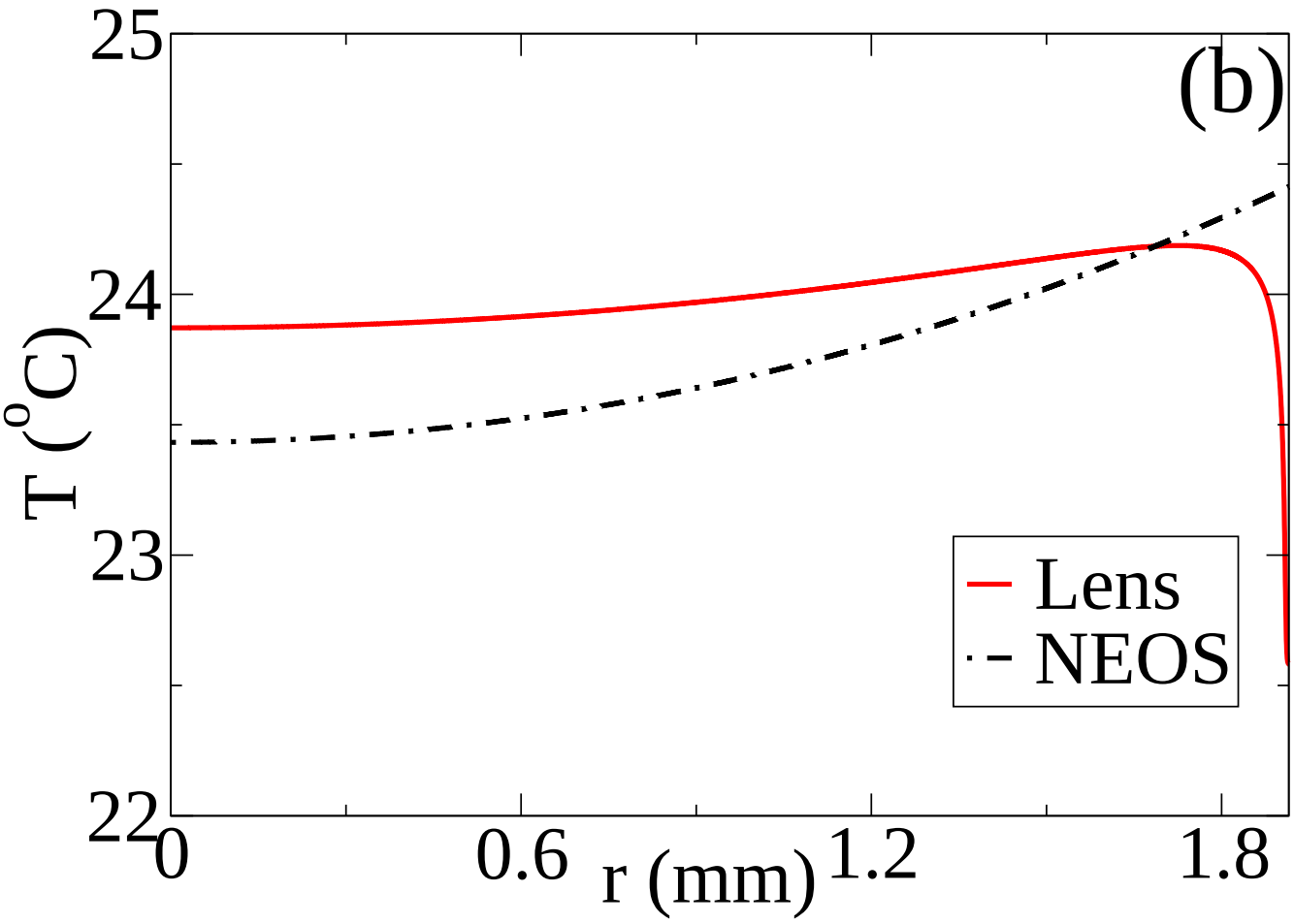

Figure 3b

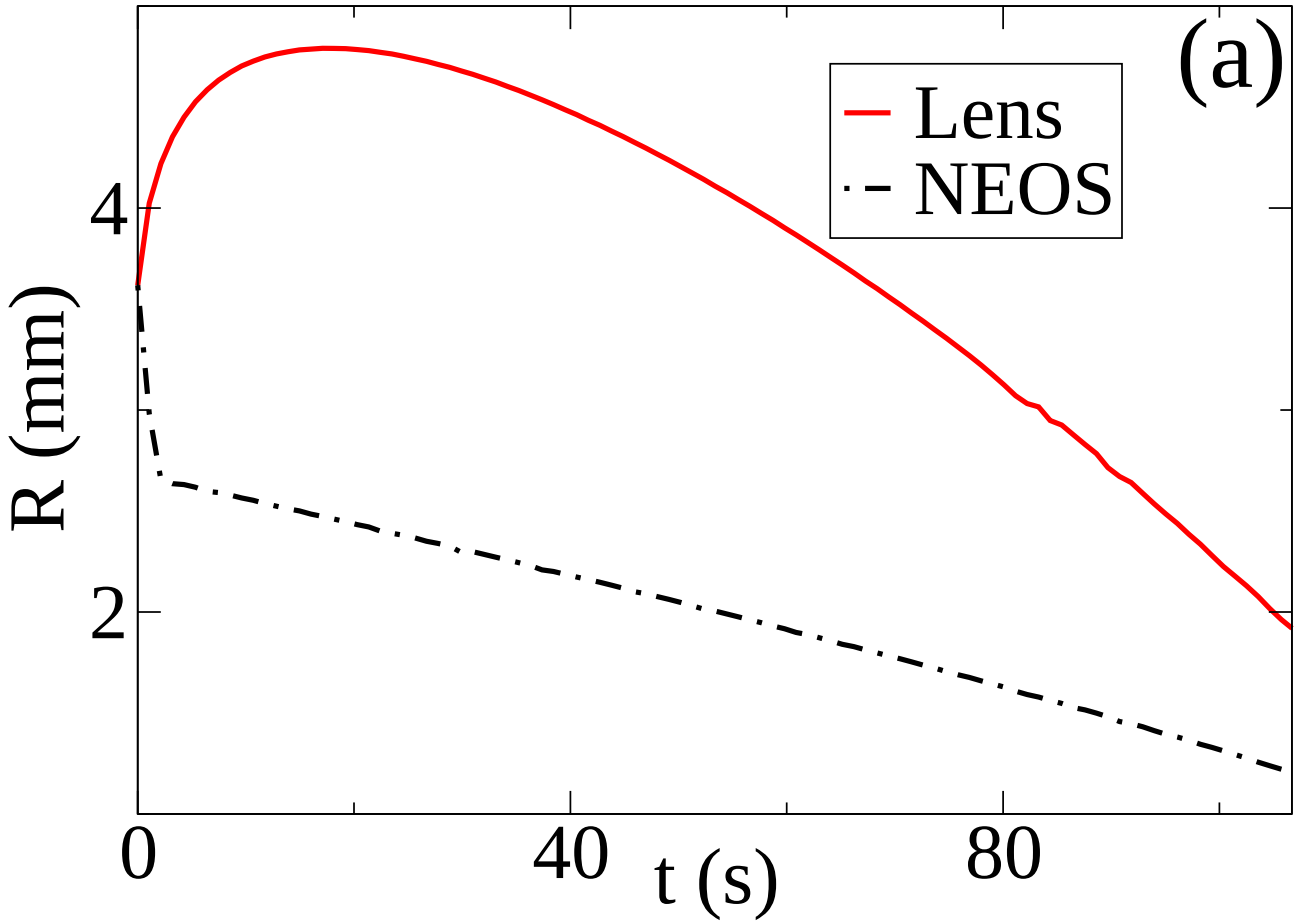

Figure 4a

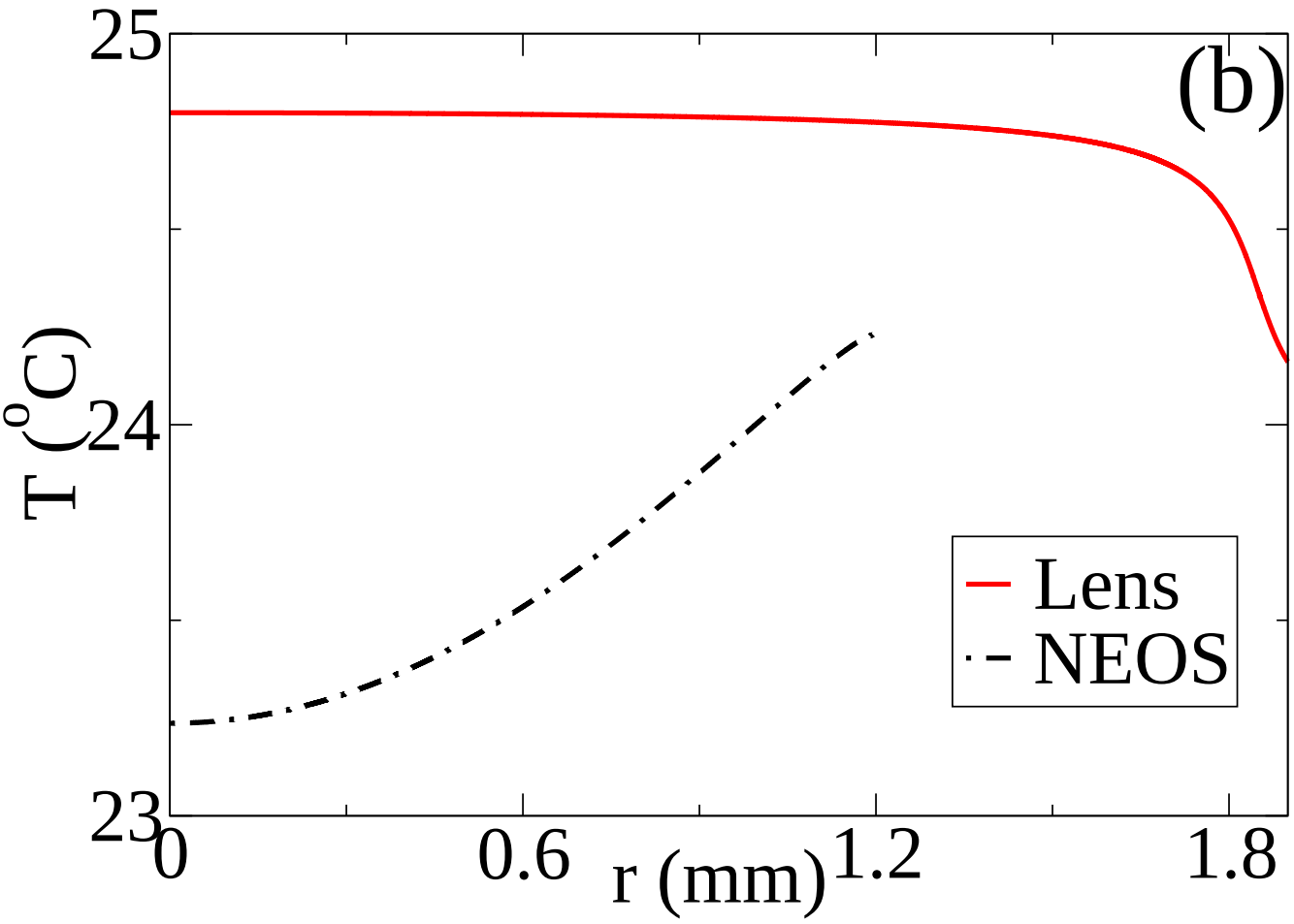

Figure 4b